

Higher sensitive influence on Cu₂S: Sb and Cu₂S: Al heterojunction for application photodetectors

H. K. Hassun ^{a,*}, B. H. Hussein ^a, B. K. H. Al-Maiyaly ^a, R. H. Athab ^a,
Y. K. H. Moussa ^b

^a *Department of Physics, College of Education for Pure Science (Ibn Al-Haitham),
University of Baghdad, Baghdad, Iraq*

^b *College of Science, University of Baghdad, Baghdad*

Photoconductive possessions through the highly sensitive and responsive in lower applications apply voltages with a charge that effect the product for the photodetector utilizing Copper Sulfide was effective to fabricate and deposit by the means of thermal evaporation techniques following by the heat treatment with applications as the visible photodetector was described. Effects of doping to the antimony and aluminum on photo detectors property were estimated to be below illumination by the utilization of different power densities. The structure with the surface morphology properties was studied by XRD and AFM techniques, a clear effect of dopant on absorption coefficient and energy gap was found in examination of the optical transmit, the device photocurrents property under reverse bias by utilizing several illuminations had been tested, moreover the high responsivity of Cu₂S: Al/Si photo detectors was around the wavelength of 751 nm, quantum efficiency besides the detectivity had been evaluated for every sample, the values of responsivity by the help of doping has risen which is required for good photodetectors application.

(Received February 20, 2025; Accepted June 20, 2025)

Keywords: Responsivity, Copper sulfide, Absorption coefficient, Sensitive influence,
Vacuum evaporation

1. Introduction

P-type optical transparency conduct materials establishes the indispensable difficulty for expansion of several optical electronics beside full electronics campaigns. Although there is a motionless difficulty to grasp higher optical transparency per the major number of the holes of conductivity through the lower mobility of the holes in comparison of electrons' which are associated. Copper Sulfide had revealed a greater promise on the expansion of the transparent conductive material constitutes [1]. Amongst Binary semiconductors for II-VI which had received important usage in photovoltaic devices., Cu₂S keeps around its special characteristic for heterojunction application per Si [2,3]. Cu₂S has direct bandgap energy besides indirect band gap for 1.2eV and 1.8eV correspondingly, and with higher holes concentration of CuS, it involved many considerations on fields for transparent conducting materials for the diversity of the optoelectronics campaigns. For example: solar cell and transparent LEDs and LED display [4-7]. In addition to electro conduct coating, solar control coating, Photovoltaics requests, and microwave shield coating, similar utilization on several fields for optical filters and ions conduction [8-10]. Cu₂S thin films had been equipped through several deposited methods. For example: spray pyrolysis, solid state reaction, vacuum evaporate, and sputtering [11-13]. Sartale and Lokhande simply described ion layers as adsorption layers besides the reacted (SILAR) technique in produced Cu_xS thin films, found the films are amorphous or contain one of the acceptable grain sizes in the glasses substrate, while countless folds upsurge the crystallinity which had been observed for Si (111) wafers substrate [14]. Also, Yahiya et al., studied the electrical and photoelectric properties for Cu₂S: Si procedures via utilization of chemical spray pyrolysis

* Corresponding author: hanan.k.h@ihcoedu.uobaghdad.edu.iq
<https://doi.org/10.15251/CL.2025.226.541>

techniques, examine the forward currents for this junction used the tunnel recombination models [15], higher rectal photo detection device had been fabricated used the chalcogenides in the place of active materials. Wang et al. have utilized the mono disperse copper antimony sulfide to manufacture hybrid photo detectors for the highest sensitivity besides stability [16]. This work focuses on the prepared Cu_2S films by the vacuum evaporation technique and studied dopant effects, the consistent modification on structural, optical and Photodetector properties for all films had approved in details.

2. Experimental details

Successful fabrication of Cu_2S alloy have utilized powder with the purity of 99.99%, thin films had been deposited in micro scope glass and Si substrate. These substrates were placed in the ultrasonic on deionized water then in isopropanol, correspondingly. They were followed via dropping the silicone substrate in 10% HF acid solution with the intention of etch the native oxide layers and rinsed through isopropanol. Later, they were cleaned, substrate besides the deposit material had been placed in the chamber of Thermionic Vacuum Arc (TVA). The method was done via the thermal evaporation technique that forms materials to be deposited. films doping through (Sb, Al) per percentage of 4% had been deposited with the thickness of 350 nm on R.T. then annealing all of the films at 473 K for 1 hour to activate the films properties then after the applications as in the optoelectronic device. The structural, morphological, optical, and electrical analysis had been approved through the assistance of X-ray diffractometer system which had recorded the intensity by the method of function for Bragg's angle, source radiate had put the Cu ($k\alpha$) through $\lambda=1.5406 \text{ \AA}$. With An atomic force microcopy of the (AA3000) type, which has a high analysis power had been used to examine the nature surface of the prepared films. Optically transmit quantities had been perform through UV-Visible Spectro photometer 1800. The band gap besides optical constant for transparent film is resolute in the optical transmission spectra. I-V characteristics had the quantity to be utilized in Farnell Instrument F30-2, with K.D electrometer 616, then complete in reverse bias voltages expose Halogen lamp light Philips through dissimilar intensity, for regulate the spectral responsively ($R\lambda$), quantum efficiency (η) and specific; detectivity (D^*) to complete the sample.

3. Results and discussion

Structural analysis include XRD shapes for the deposited Cu_2S thin film purity of 4% Al and Sb doped films as in the Figure (1) , the indicative peaks exhibited the procurement of (Cu_2S) through cubic crystal structure and reduction in the width of peaks after doping where observed and that is attributable to the entrance of ions of the impure material in the crystal structure of the material and the spread of ions within the crystal lattice of Cu_2S and the new peaks of dopant films had low intensity of crystal levels in addition to the occurrence of displacement which is very few towards the lower angles in peaks after doping .

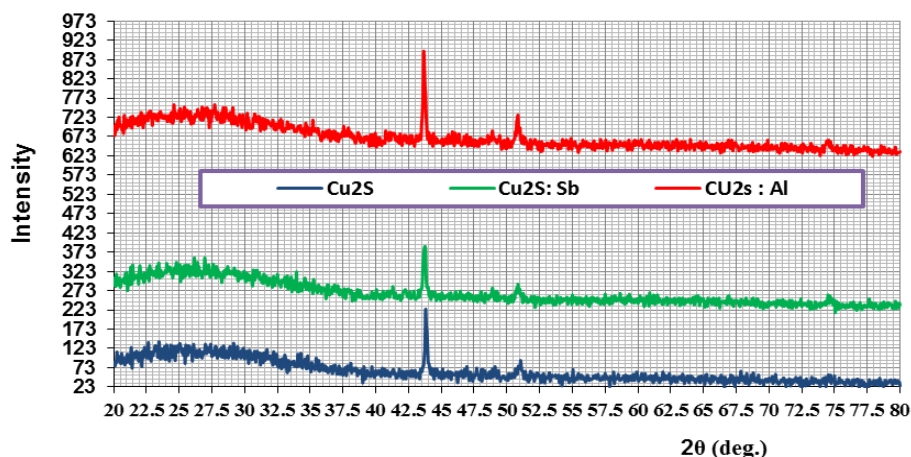


Fig. 1. XRD for thin films of Cu_2S pure and 3% ratio Sb, Al at (473K).

Rendering for Scherrer's equivalence crystallite size $C.S$ had resolute as [17], and dislocation density δ [18].

$$C.S = \frac{0.94 (\lambda)}{\beta \cos \theta} \quad (1)$$

$$\delta = \frac{1}{(C.S)^2} \quad (2)$$

where λ was wavelength radiation, FWHM was fullwidth, half maximum for main peak and θ is the diffraction angle. Table 1: displays results gotten from pure the doping of films, we distinguished the effect of doping and annealing where the increase in the crystal size of the (Cu_2S) thin film equipped after dopant [19], which principals' diminution in dislocation density and stress besides enhanced crystalline properties after doping and annealing.

Table 1. XRD decorations of (Cu_2S) thin films pure and doped in 473K.

Thin film for hkl (220)	Cu_2S	Cu_2S : 4% Sb	Cu_2S : 4% Al
C.S (nm)	44.87	53.32	58.88
δ (nm^{-1})	0.000496	0.000351	0.000288

Atomic force microscope device has been used to determine the topography of the surface films, studying the consequence of distortion and surface roughness values with effect of (Sb, Al) dopant. Figure (2) and Figure (3), illustrate the AFM results for all the prepared films, where all surfaces are regular, homogeneous, and connected regularly without the presence of interstitial cracks, voids, or holes in the structures. An increase in the values average grain size and surface roughness was found in the case of the film doping through Al and that is attributed to the occupancy of the atoms' impurities sites within the crystal lattice and this is consistent with the results of XRD which indicates the improvement of structural properties after doping and annealing [20, 21].

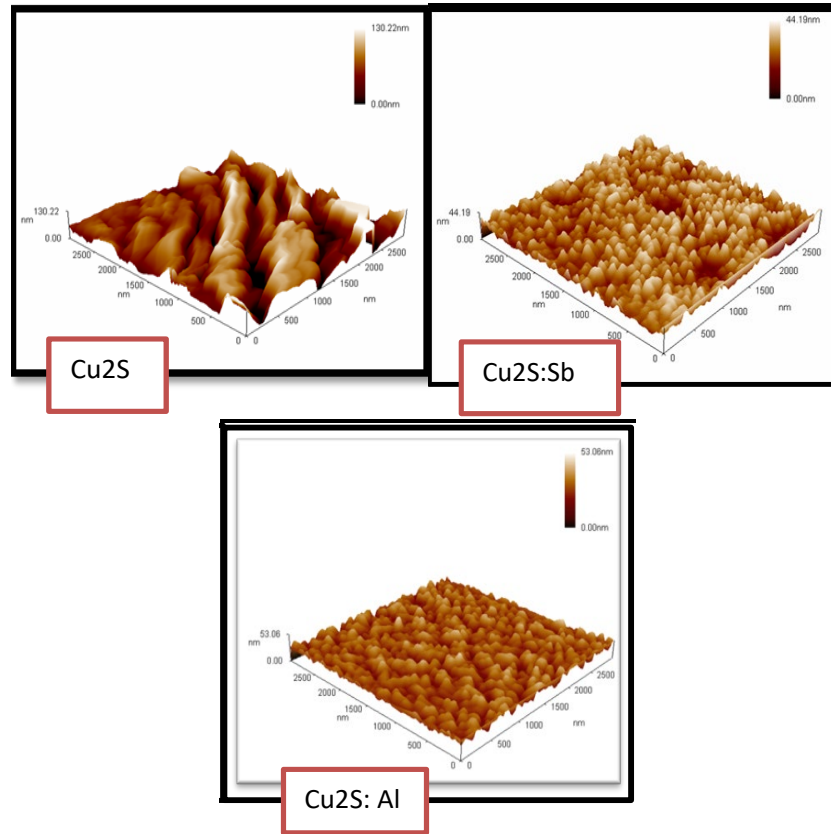


Fig. 2. AFM imageries for (Cu_2S) thin films pure and doped at 473K.

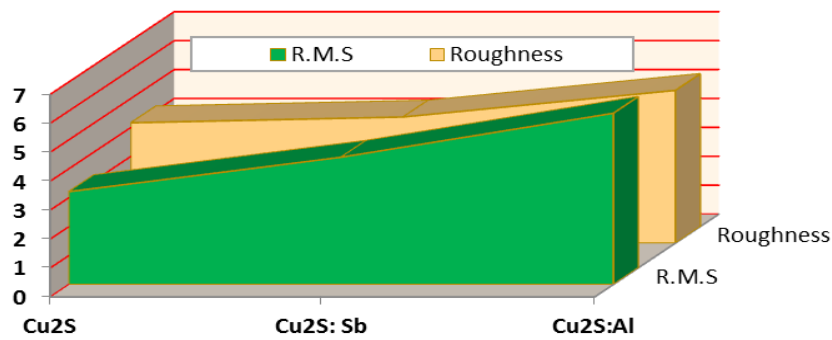


Fig. 3. Roughness and R.M.S for (Cu_2S) thin films per effect dopant at 473K.

The absorptive coefficient (α) and the bandgap (E_g) had been considered since the transmitted spectrum which is utilized in Tauc equation as in the relation [22].

$$(\alpha h\nu) = D (h\nu - E_g^{opt})^r \quad (3)$$

whenever Plank's constant is (h), frequency for incident photon is (ν), then D constant. Values r colleagues toward 2 allowed directs, $1/2$ for allow indirect besides $2/3$ for a forbidden transition. Strong absorbance is shown in figure (4) in the variety of 300 to 900 nm then had been decreasing for the highest wavelength was strong in the assumed spectra due to that high absorption in region (630-850) nm. Also, Cu_2S films have high absorption coefficient values ($\alpha > 10^4 \text{ cm}^{-1}$), which means that direct electronic transitions are allowed. Furthermore, the absorption coefficient values of all films increased through photons energy. In addition, we noticed the effect of doping for

increasing the absorption coefficient with 4% (Sb, Al) and the reason for that is the distortion presented in the secondary levels within the energy gap, which increases electronic transfers, in addition to the transitions of carriers between energy band, and this leads to an increase in the absorption process and the absorption coefficient.

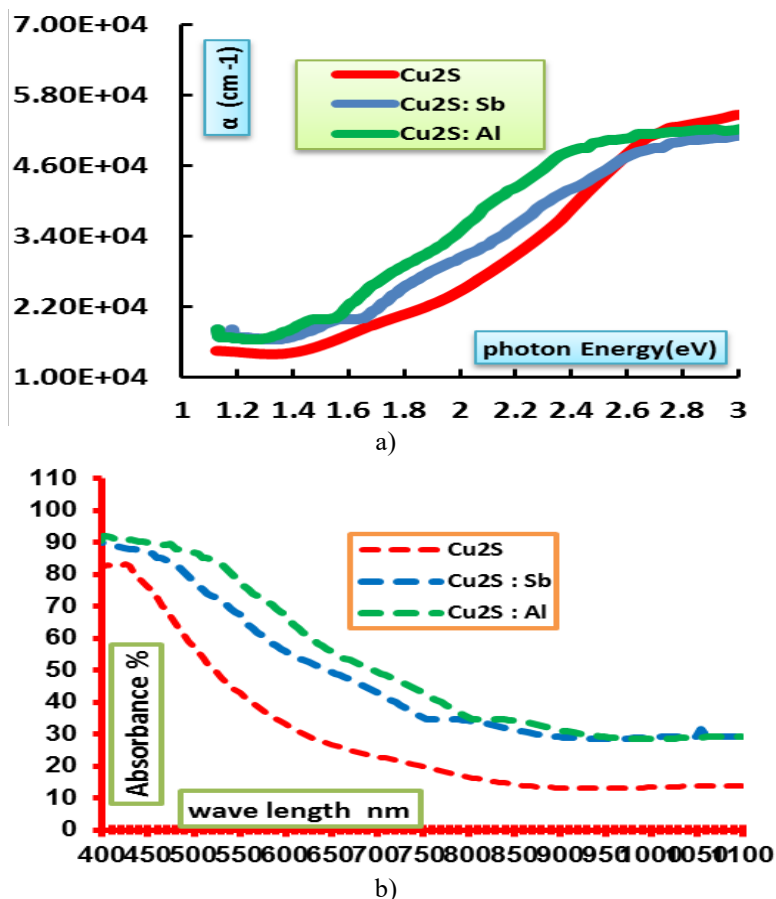


Fig. 4. (a) Optical absorption spectra and (b) absorption coefficient for (Cu₂S) thin films then effect dopant at 473K.

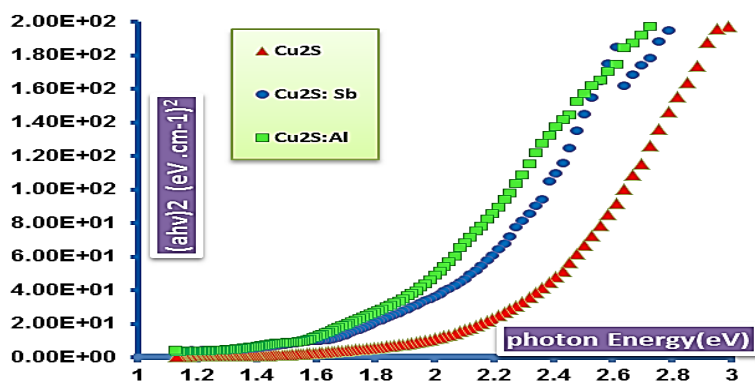


Fig. 5. $(ah\nu)^2$ plus photons energy for (Cu₂S) thinfilm beside effects dopant in 473K.

The rate of the direct energy gaps of the prepared dopant (Cu_2S) films with (Sb, Al) had been intended after the process of annealing by drawing a graphic relationship within $(\alpha h\nu)^2$ via the incident photons energy. Figure (5) expression the process of dopant and annealed led to reduction on the standards of energy gap of Cu_2S thin films which were (2.15eV) to (1.65eV), where the formation of new levels within the energy gap within valence and conduction beams, so the energy gap values appear less after doping.

I-V properties by way of role for the forward. Besides, reverse bias voltage for junctions ($\text{Cu}_2\text{S}/\text{Si}$), ($\text{Cu}_2\text{S}:\text{Sb}/\text{Si}$), and ($\text{Cu}_2\text{S}:\text{Al}/\text{Si}$) with effect of annealing were revealed on Figure(6) where they had effects on the dark current and illumination in the case of front and reverse bias, as shown in the figure, we observed weak current at low voltages in the case of forward bias, charge carriers passing through the junction will increase due to the defects that arise in the interfacing between the two materials that make up the heterojunction, therefore it has growth with the external voltage applied to both sides of the junction, followed by a rise of an exponentially increasing current per voltage, the electric field increasing made upsurges in the speed drift carriers. I-V characteristics in reverse bias show the current gain and exponentially on forward bias, while in currents had been increasing a little through voltage, the forward current had binary regions behaves for entirely detectors, the currents were indistinguishably minor, where current had recombination current [21]

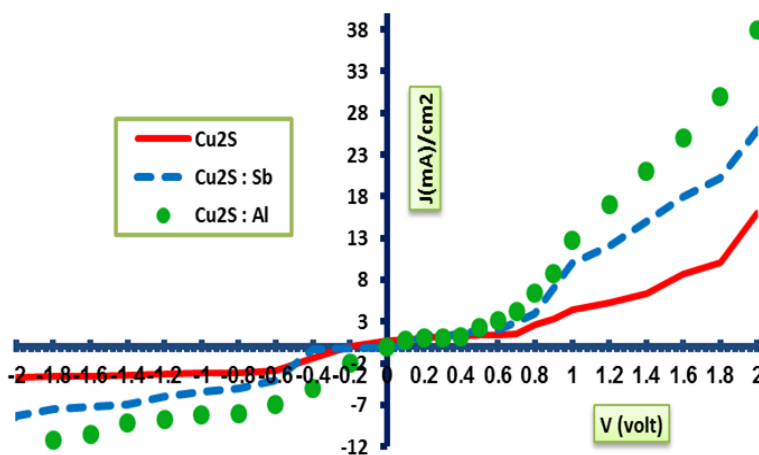


Fig. 6). I-V characteristics for ($\text{Cu}_2\text{S}/\text{Si}$), ($\text{Cu}_2\text{S}:\text{Sb}/\text{Si}$) besides ($\text{Cu}_2\text{S}:\text{Al}/\text{Si}$) heterojunction.

Under illumination approves through light absorption, charge carrier generation and transported foremost toward growth in photocurrent associated with dark, defects were private in the energy gap levels also the internal of depletion region performance via income of recombined centers formerly incentive reduction current moves.

Figure (7) shows the (I-V) characteristics of the $\text{Cu}_2\text{S}/\text{Si}$ detectors with divergent incidence power density (86,155, 230) mW/cm^2 dark and light illumination state. The increase in the photo current was attributable to the drift velocity of generating electron, the photo currents on the reverse direction had been powerfully amplified through photo illumination, the currents which had reverse direct was strongly improved via lighting. This behavior produces beneficial data for electro hole pairs generated through incidental photons, photocurrents was higher than dark currents for similar or reverse bias. While illuminated junction the additional carrier was generated. Moreover, for forward currents rises. Similarly, illuminate junction amplified by reverse bias currents by way of expectable meanwhile electrons hole pair generated at a depletion region, uncertainty the amount of photons energy was greater than the lower direct band gap for the heterojunction, also doping percentage made the optical energy gap reduction a desirable condense electrically resistive which results in the increase of the concentration of carriers when adding around mobility besides that styles the light currents enhanced over collective Al doping proportion.

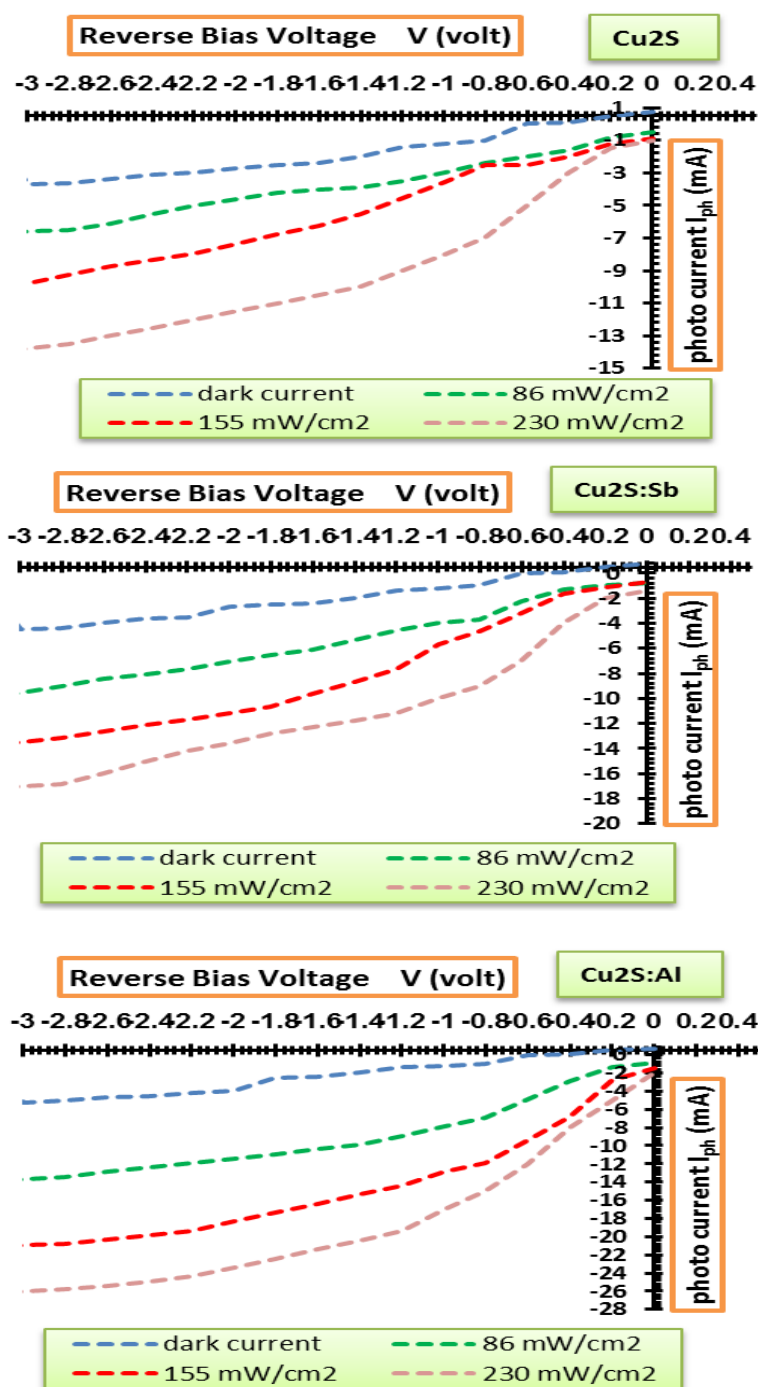


Fig. 7. I-V characteristic for $\text{Cu}_2\text{S}/\text{Si}$ heterojunction at pure besides dopant (Sb,Al) plus varied incident power density.

The disparity of Responsivity (R_λ) and specific detectivity (D^*), explain with comparison [23,24], demonstration in figure (8) revealed the extreme photoresponsivity peak of $\text{Cu}_2\text{S}/\text{Si}$ detectors at pure besides (Sb, Al) doping (biased at 4 V) rang (530 to 800) nm. the samples had good response in the visible region, besides highest responsivity peak around (567-750) nm for $\text{Cu}_2\text{S:Al}/\text{Si}$ sample, where rendering the band gap (1.65 eV), highest intensity and robust responded on lengthy wavelength had appear, the response intensity had improved with dopant content with Cu_2S films [25], decrease band gap with effects annealed make radically growth of lights absorption formerly rise carrier concentrate. Likewise, the specific detectivity had developed with

doping attributed for increasing on absorptive incidents radiate for thin film where had generated electron holes pair.

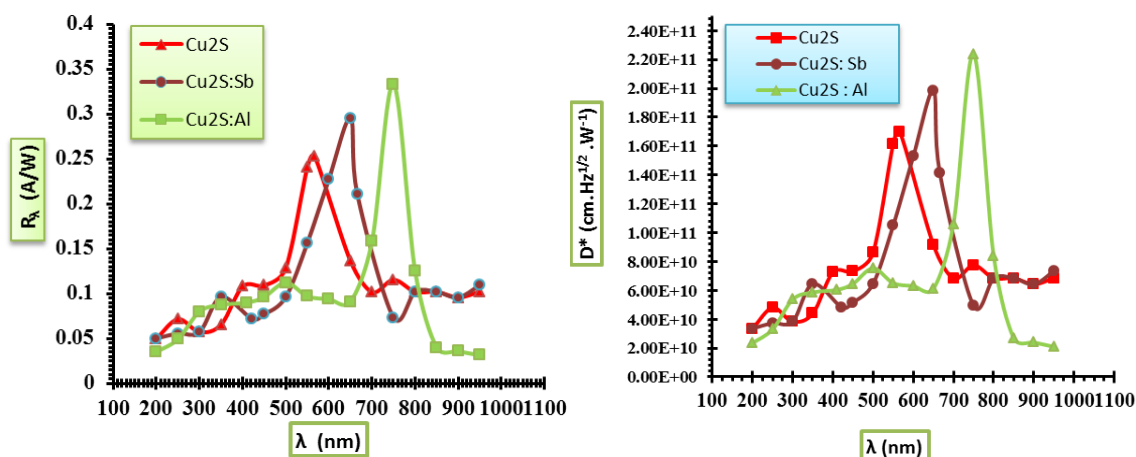


Fig. 8. Responsivity (R_λ) and specific detectivity (D^*), pointed at for Cu₂S/Si photodetectors with effect doping.

The quantum efficiency of the doped and undoped Cu₂S/Si photodetectors had quantity as purposes for incident light were demonstrated at figure (9), to conclude things, dopant shows increased values due for rising at the absorptive incidents radiation for films which had generated electron hole pairs, besides, as a result of increased spectral responsivity with diminutions noise equivalent power (NEP), the smallest NEP happens once responsivity had the extreme value as show in figure(10), the NEP reductions effected with dopant atoms by reason of diminution noise current.

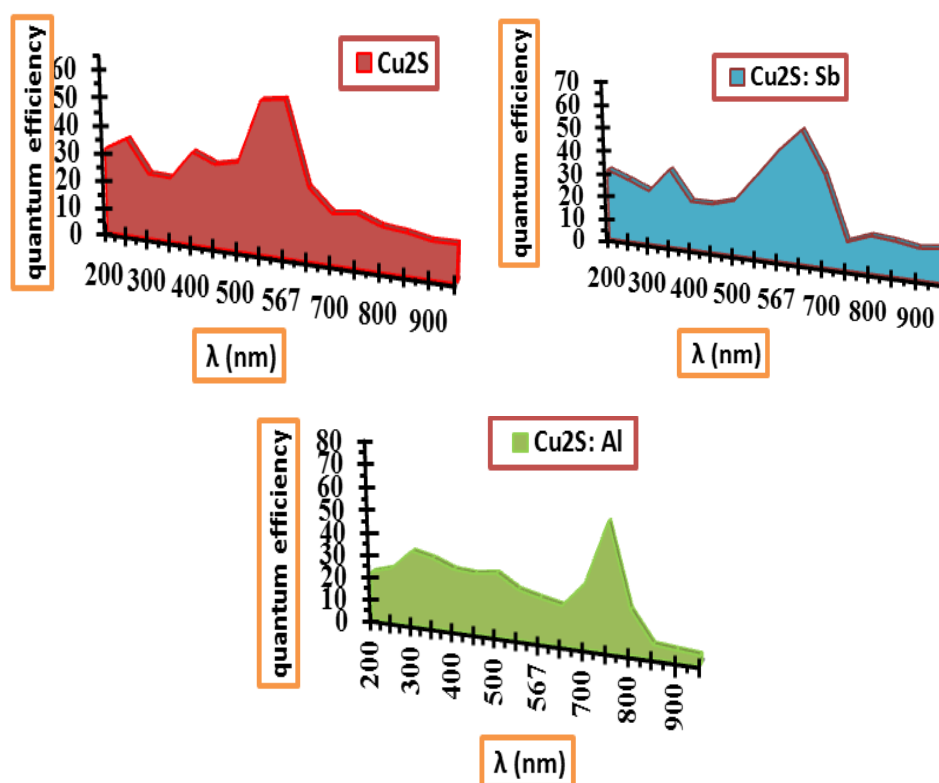


Fig. 9. Quantum efficiency for Cu₂S/Si photodetectors with effect doping.

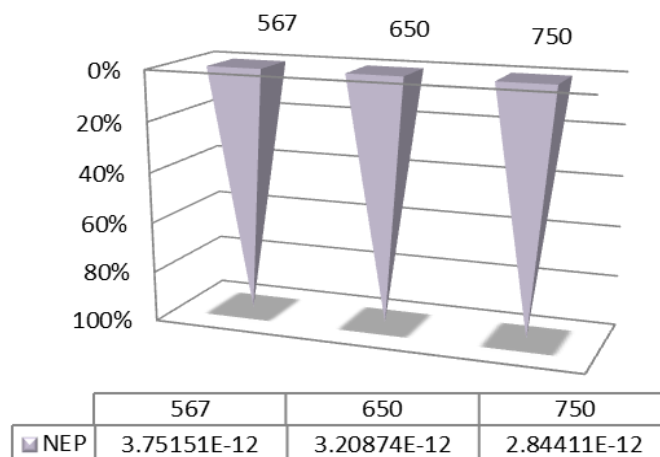


Fig. 10. Dissimilarity noise equivalent power (NEP) over wavelength for $\text{Cu}_2\text{S}/\text{Si}$ photodetectors with effect doping.

4. Conclusions

In summary, we fabricated and characterized $\text{Cu}_2\text{S}/\text{Si}$ thin films-based photodetectors utilizing thermal evaporation technique. The as deposited thin films doped with Sb, Al per percentage 4% had then be submitted through an annealing proses.

The structure and morphology and opto-electronic properties of the $\text{Cu}_2\text{S}/\text{Si}$ with special focus on the photo detection application were investigated in detail. From the structure and morphology properties we have observed a regular and homogeneous surface and an increasing in the crystal size (Cu_2S) of the doped thin films.

The optical transit showed direct electronic transitions and the formation of new levels within the energy gap from the valence and then conduction bands, therefore, the energy gap values appear less after doping.

I-V measurements presented distinctive correcting performance, under illumination the photocurrent rises with dopant effects, where the light currents enhanced over collectives Al doping proportion.

The maximum responsivity was observed for all samples. Also, high values of specific detectivity and quantum efficiency were recorded for the aluminum dopant atom,

This existing study on rate-efficient products for photodetector devices, through the selected wavelength, has presented detection characteristics and advantages at the lowest possible cost and using friendly materials.

References

- [1] M. Adelifard, H. Eshghi, M.M.B. Mohagheghi, Appl Surf Sci. 258 (15) (2012), 5733-5738; <https://doi.org/10.1016/j.apsusc.2012.02.079>
- [2] H.S. Soliman, A.A.M. Farag, M.M. Saadeldin, K. Sawaby, Acta Physica Polonica A No. 6, Vol. 127 (2015).
- [3] C. Papadopoulos, Solid State Electronic Devices, Springer, New York 2014; <https://doi.org/10.1007/978-1-4614-8836-1>
- [4] I. Popovici, L. Isac, A. Duta, Bulletin of the Transilvania University of Brasov 2 (51), (2009) 193-196.
- [5] Zhang Y, Xu X, Fang X., InfoMat. (2019); 1:542-551; <https://doi.org/10.1002/inf2.12035>
- [6] Xu, X., Shukla, S., Liu, Y., Yue, B., Bullock, J., Su, L., Li, Y., Javey, A., Fang, X., Ager, J.W. (2018), Phys. Status Solidi RRL, 12: 1700381;

<https://doi.org/10.1002/pssr.201700381>

[7] Xu, X. J., Chen, J., Cai, S., Long, Z., Zhang, Y., Su, L., He, S., Tang, C., Liu, P., Peng, H. S., Fang, X. S. Photodetector Adv. Mater. 2018, 30, 1803165;

<https://doi.org/10.1002/adma.201803165>

[8] Yamamoto, T., Kubota, E., Taniguchi, A., Dev, S., Tanaka, K., Osakada, K. Sumita. M.

(1992), Chem. Mater., 4, 570-576; <https://doi.org/10.1021/cm00021a015>

[9] Nair, M. T. S., Nair, P. K. (1989). Semicond. Sci. Technol., 4, 191-199;

<https://doi.org/10.1088/0268-1242/4/3/009>

[10] Tang, K., Chen, D., Liu, Y., Shen, G., Zhang, H., Qian, Y. (2004). Journal of Crystal Growth, 263, 232-236; <https://doi.org/10.1016/j.jcrysgro.2003.11.045>

[11] Wang, S. Y., Wand, W., Lu, Z. H. (2003). Mater. Sci. Eng., B, 103, 184-188;

[https://doi.org/10.1016/S0921-5107\(03\)00199-5](https://doi.org/10.1016/S0921-5107(03)00199-5)

[12] He, Y. B., Polity, A., Österreich, I., Pfisterer, D., Gregor, R., Meyer, B. K., Hardt, M.

(2001). Physica B, 308-310, 1069-1073; [https://doi.org/10.1016/S0921-4526\(01\)00851-1](https://doi.org/10.1016/S0921-4526(01)00851-1)

[13] Ramya, M., Ganesan, S. (2012). Journal of Optoelectronics and Advanced Materials, 14, 910-917.

[14] S.D. Sartale, C.D. Lokhande, Mater. Chem. Phys. 65, 63 (2000);

[https://doi.org/10.1016/S0254-0584\(00\)00207-8](https://doi.org/10.1016/S0254-0584(00)00207-8)

[15] C. Song, H. Yin, N. Zhang, S. Li, B. Zhao, K. Yu, Mater. Lett. 137, 56 (2014);

<https://doi.org/10.1016/j.matlet.2014.08.117>

[16] J.-J. Wang, Y.-Q. Wang, F.-F. Cao, Y.-G. Guo, L.-J. Wan, J. Am. Chem. Soc., 2010, 132,

12218-12221; <https://doi.org/10.1021/ja1057955>

[17] Samir A Maki, Hanan K Hassun, IOP Conf. Series: Journal of Physics: Conf. Series 1003

(2018) 012085; <https://doi.org/10.1088/1742-6596/1003/1/012085>

[18] H. K. Hassun, M. H. Mustafa, R. H. Athab, B. K. H. Al-Maiyaly, B. H. Hussein, Journal of Ovonic Research Vol. 18, No. 4, 2022, p. 601 – 608;

<https://doi.org/10.15251/JOR.2022.184.601>

[19] Hanan K. Hassun, Bushra H. Hussein, Bushra K.H. Al-Maiyaly, Auday H. Shaban, Key Engineering Materials, Vol. 886, pp 66-74, 2021;

<https://doi.org/10.4028/www.scientific.net/KEM.886.66>

[20] B. K. H. AL-Maiyal, Ibn Al-Haitham J. for Pure & Appl. Sci 26(1) (2013).

[21] H.S. Solimana, A.A.M. Faraga;b;, M.M. Saadeldinc, K. Sawaby, Acta Physica Polonica A, No. 6, Vol. 127 (2015); <https://doi.org/10.12693/APhysPolA.127.1688>

[22] Samir A. Maki Hanan K. Hassun, Ibn Al-Haitham J. for Pure & Appl. Sci. Vol.29 (2) 2016.

[23] Hanan K. Hassun, Bushra H. Hussein, Ebtisam M.T. Salman, Auday H. Shaban, Energy Reports 6 (2020)46-54; <https://doi.org/10.1016/j.egyr.2019.10.017>

[24] H. K. Hassun, B. K. H. Al-Maiyaly, B. H. Hussein, Y. K. H. Moussa, Journal of Ovonic Research Vol. 19, No. 6, 2023, p. 719 – 726;

<https://doi.org/10.15251/JOR.2023.196.719>

[25] M. Hao, Y. Liu, F. Zhou, L. Jiang, F. Liu, J. Li, ECS Solid State Lett., 2014, 3, Q41-Q43;

<https://doi.org/10.1149/2.0011409ssl>

[26] S. Bulyarsky, L. Vostretsova, S. Gavrilov, Semiconductors, 2016, 50, 106-111;

<https://doi.org/10.1134/S1063782616010061>

[27] R. Guo, T. Shen, J. Tian, J. Mater. Chem. C, 2018, 6, 2573- 2579;

<https://doi.org/10.1039/C8TC00288F>